Journal of Solid Mechanics Vol. 12, No. 4 (2020) pp. 774-790
DOI: 10.22034/jsm.2020.1864464.1411

ANSYS Modeling for Bone Reconstruction by Using Hybrid Nano Bio Composite

J. Sattar Kashan, S. Mahmood Ali *

Biomedical Engineering Department, University of Technology, Baghdad, Iraq

Received 7 July 2020; accepted 12 September 2020

ABSTRACT

In the present work, an attempt has been made to study and improve the physical and biomechanical properties of adding Titanium dioxide (TiO_2) and yttria stabilized zirconia (Y-PSZ) Nano fillers ceramic particles for reinforced the high density polyethylene (HDPE) matrix Nanocomposites for fabricated six bio nanocomposites hybrid by using hot pressing technique at different compounding temperature of (180,190, and 200 °*C*) and compression pressures of (30, 60, and 90 *MPa*). The fabricated Nano systems were designed, produced and investigated for use in repairs and grafting of the human bones, which are exposed to accidents or life-threatening diseases. The main current research results show that with the increase of the TiO_2 filler contain from 0 to 10 %, the value bulk densities increase by 30.24 % and when adding 2% partial stabilized zirconia (Y-PSZ), this value was further increased by 13.91%. For the same conditions the value percentages true porosity decrease by 48.68 % and further by 84.85 %, respectively. For the same previous parametric values, it has also been accessed that the maximum compression strength for this study was increased by 33.34 % and then further by 22 %, where these values higher by 90.11% than the previous mentioned studies. The micro-Vickers Hardness increased by 30.11 % for the second manufacturing system comparing with the first one, while the maximum equivalent von–Misses Stresses obtained from the current work withstand higher stresses than the natural bone by 52.65 higher than the previous studies. The stress safety factors increase by 58.38 % and by 21.42 % for the first and second systems, respectively. The achieved results values for the modeled femur bone is equivalent to actual service of the activity during normal movement of the patient. These results give great the designers choices to use successful bio composites for in vivo tests according to the clinical situation, age and the static and dynamic loads when designing a material to repair the fractured bones due to different types of accidents.

Keywords: Femur bone ANSYS modeling; Nano HDPE /ceramic Bio-composites; Titanium Oxide; Yttria stabilized zirconia (Y-PSZ); Bone biomechanics.

1 INTRODUCTION

BONES in the human body are a living natural composite material, fractured due to impact stress and excessive loads [1-2]. They have a complex microstructural feature [3-4]. The effects of filler nanoparticles on these properties have been extensively investigated in recent years [5]. It has been found that the addition of a few

*Corresponding author. Tel.: +96 47803700877.
E-mail address: 30249@uotechnology.edu.iq (S. Mahmood Ali).

percent of these nanoparticles can result in significant improvement in physical and chemical properties [6]. The main scaffolds materials can be categorized: polymeric, ceramic, composite, and metallic scaffolds [7-8]. The interaction of ceramic particulates with a thermoplastic high-density polyethylene (HDPE) material was consider as a very important factor influence on the tensile strength and fracture behavior of the HDPE- zirconia composites, which has formed the basis for selecting the Nano particles for bio-composite materials engineering [6]. In recent years, the adding small percentages of inorganic Zirconium dioxide (ZrO_2), also known as yttria (Y_2O_3), and titanium dioxide (TiO_2) with synthesized polymer Nano composites have been increasing due to their significant improvement in their thermal stability, electrical properties and mechanical performance [5, 9-11]. Titanium and its alloys, including the titanium oxide (TiO_2) are superior to many biomedical materials, such as stainless steel. They are widely used as orthopedic and implant materials for their biocompatibility and excellent mechanical properties, resistance to corrosion, absence of cytotoxicity, inertness and compatibility [12-13]. During melting, the polymerization process affected the polymer becomes viscous and its chains grow longitudinally and, the monomer remains relatively mobile due to the exothermic and the release of heat of the polymerization rate. The highly nonlinearity of the reaction rate during the process makes it difficult to capable of supporting stress. The problem is simplified if the mechanism of stress can be considered as a result of thermal deformations only. Results show maximum tensile stresses normal to the cracks directions, due to a link between residual stress and preload cracking [14]. To study the mechanical behaviour of biological structures, the finite element analysis (FEA) has been increasingly adopted [15-20], using the 3D finite element Analysis (FEA) to investigate the effect of daily living activity loading conditions on the mechanical strength in human bone [21-26].

The main objectives of this work were to predicted the influence of adding different concentrations of titanium dioxide and partial stabilized zirconia (PSZ) Nano ceramic fillers powders with at different compression pressures and compacting temperatures using the hot pressing fabricating technique on the physical and mechanical properties for TiO_2/ HDPE and Y_2O_3- partial stabilized zirconia (Y-PSZ)/ TiO_2/ HDPE Nano composites systems and to investigate the highest stress factors of safety to withstand the daily human activities loads. The SOLIDWORKS and ANSYS modeling were used to simulate and predicted the fracture mechanical behavior of the femur bone by develops a 3D solid numerical model, with the use of finite element method (FEM) for the human femur bone corresponding to the patient activities. The response surface methodology (RSM) technique and the Design Expert software program were used to improving and verifying the results, reaching and evaluated the optimal thermal and mechanical properties.

2 MATERIALS AND METHODS

2.1 Nano composites preparation method

Six Nano composites systems TiO_2/ HDPE and Y_2O_3- partial stabilized zirconia (Y-PSZ)/ TiO_2/ HDPE were fabricated in this study and used as bone grafting bio-composites. The used ceramic fillers are; the 99% purity titanium dioxide (TiO_2) with a particle density of 4.23 g/cm^3 and an average particle size of 40 *nm*, imported from M.K Nano (Canada, Toronto) and the 99.9% purity partially-stabilized zirconia (ZrO_2-PSZ), doped with 3 mol. % of yttria (Y_2O_3), of 5.91 g/cm^3 density and an average particle size of 40 *nm*, imported from M.K. Nano (Canada, Toronto). The particle size of 5 μm and density of 0.95 gm/cm^3 used high-density polyethylene (HDPE) biomaterial powder matrix was supplied by the Right Fortune Industrial Limited (China, Shanghai).

The prepared powders mixtures with each desired composition were dry mixed in a ball mill machine for 12 *hrs*, and then hot pressed at 180, 190, and 200 $°C$ and using a compounding pressure of 30, 60, and 90 *MPa*, respectively. The produced test samples were of a cylindrical shape with a height between 3 and 5 mm and 10 mm diameter. The main properties of the used nanomaterials are given in Table 1.

Table 1
The main properties of the used bioactive nanomaterials [27].

Property	Titanium dioxide	Zirconium dioxide (Zirconia)	Yttrium oxide (Yttria) or Yttrium (III) oxide	High density polyethylene (HDPE) matrix
Chemical formula	TiO_2	ZrO_2	Y_2O_3	C_2H_4
Molar mass (*g/mol*)	79.87	123.22	225.81	1000
Appearance	White solid	White powder	White solid	Translucent to White
Density (g/cm^3)	4.23	5.68	5.01, solid	0.94 - 0.97
Melting point ($°C$)	1843	2715	2425	126
Boiling point ($°C$)	2972	4300	4300	> 300
Young's modulus (*E*) (*GPa*)	230-288	210	120	1.04

Tensile strength (σ_t) (*MPa*)	333.3-367.5	88-1500	-	19
Endurance Limit (*MPa*)	283.5-330.7	107-640	-	-
Compressive Strength (*MPa*)	660-3675	1990	390	20
Shear Modulus (*GPa*)	90-112.5	77.8	61	0.21
Fracture Toughness (KIC) ($MPa.m^{1/2}$)	2.4-3.3	6.4-10.9	9-10	1.52-1.82
Poisson's Ratio	0.27-0.29	0.3	0.31	0.40 - 0.45
Thermal Expansion ($10^{-6}/K$)	8.4-11.8	10	8	2. 0
Solubility	Not soluble in acidic	Soluble in HF, and hot H2SO4	Soluble in alcohol acid	Insoluble in most organic solvents
Solubility in water	Insoluble	Negligible	Insoluble	Insoluble
Thermal conductivity (*W/m. K*)	4.8, 11.8	1.7-2.7	27	0.29 - 0.48

2.2 Physical and mechanical properties testing

A disk-shaped sample, were prepared for measured the fracture strengths by using the diametrical compression tests on the Instron tensile machine with a crosshead speed of 5 $mm\ min^1$. In this test, a disk specimen is loaded along a diameter in compression edgewise. A biaxial stress state generates in the specimen with a transverse tensile stress and a compressive principal stress in the direction of loading. For a significant fraction of the test specimen, these stresses are nearly constant near the center of the disk. The following formula is used to calculate fracture strength [28]:

$$\sigma_f = 2P/\pi\ D.\mathrm{t} \quad (1)$$

where: σ_f is the tensile fracture strength (*MPa*); *P* is the crosshead load (*N*); *D* is the specimen diameter (*mm*) and *t* is the specimen thickness (*mm*).

The Vickers micro-hardness tests were carried by using the Digital Micro Vickers Hardness Tester type TH714, manufactured by the Beijing TIME High Technology Ltd. /China) using a pyramid indenter with applied load of (50*gm*). For all samples, the live bulk densities were done by using the Pycnometer instrument of sort AccuPyc1330 Pycnometer produced by the Micromeritics Instrument Corporation, Holland. The tests were performed after to remove moisture by drying the samples in oven for 48 *hr* at a temperature of 60 °*C*. Then the samples weighted by using 4-digit balances. The densities of the samples were calculated by using the Archimedes method and the following equations [28].

$$\text{Bulk density} = (W_D/W_a\text{-}W_b) * D \quad (2)$$

$$\text{Bulk volume} = (W_D/W_a\text{-}W_b) * D \quad (3)$$

$$\text{Apparent solid volume} = (W_D\text{-}W_b/D) \quad (4)$$

$$\text{Apparent solid density} = (W_D/W_D\text{-}W_b) * D \quad (5)$$

where: W_a is the weight of test piece soaked and suspended in air; W_b is the weight of test piece soaked in water and suspended in distilled water and W_D is the weight of test piece. The sintered samples are soaked in distilled water for 1 *hr* before measurement.

The True porosity was calculated using the following relation:

$$\text{True porosity } (\%) = [1\text{-bulk density/true density}] * 100 \quad (6)$$

2.3 Mathematical modeling

The governing equation used in the simulation of the femur bone consists of the geometric equation, the stress equilibrium equations, and constitutive equations. In index notation, these equations are [19]:

$$\rho \frac{\partial^2 u_i}{\partial t^2} - \sigma_{ij,j} = f_i \qquad (i=1,2) \tag{7}$$

$$\varepsilon_{ij}(u) = \frac{1}{2}\left(u_{i,j} + u_{j,i}\right) \tag{8}$$

$$\sigma_{ij} = \left(C_{ep}\right)_{ij} \varepsilon_{ij}, \tag{9}$$

where; σ and ε denote the stress, and strain respectively, u is displacement, f_i represents body force, C_{ep} is the constitutive matrix. To solve the problem boundary value, the finite element analysis (FEA) is used. The standard weighted residual technique is applied and the typical domain is denoted by Ω. Eqs. (1), (2), and (3) can be written as:

$$\rho \frac{\partial^2 u}{\partial t} - \left(\frac{\partial \sigma_x}{\partial x} + \frac{\partial \sigma_{xy}}{\partial y} \right) = f_x \tag{10}$$

$$\rho \frac{\partial^2 v}{\partial t} - \left(\frac{\partial \sigma_{xy}}{\partial x} + \frac{\partial \sigma_y}{\partial y} \right) = f_x \tag{11}$$

where,

$$\varepsilon_x = \frac{\partial u}{\partial x}, \varepsilon_y = \frac{\partial v}{\partial y} \quad \text{and} \quad \varepsilon_{xy} = \frac{\partial u}{\partial y} + \frac{\partial v}{\partial x} \tag{12}$$

and,

$$\begin{bmatrix} \sigma_x \\ \sigma_y \\ \sigma_{xy} \end{bmatrix} = \begin{bmatrix} d_{11} & d_{12} & 0 \\ d_{21} & d_{22} & 0 \\ 0 & 0 & d_{33} \end{bmatrix} \begin{bmatrix} \varepsilon_x \\ \varepsilon_y \\ 2\varepsilon_{xy} \end{bmatrix} \tag{13}$$

By using the terms of the displacements u and v in Eqs. (10) and (11) and by substituting Eq. (12) into (13) [24], then the result can be obtained in the following equations:

$$-\frac{\partial}{\partial x}\left(d_{11} \frac{\partial u}{\partial x} + d_{12} \frac{\partial v}{\partial y} \right) - \frac{\partial}{\partial y}\left[d_{33} \left(\frac{\partial u}{\partial x} + \frac{\partial v}{\partial y} \right) \right] = f_x - \rho \frac{\partial^2 u}{\partial t^2} \tag{14}$$

$$-\frac{\partial}{\partial x}\left(d_{33} \frac{\partial u}{\partial y} + \frac{\partial v}{\partial x} \right) - \frac{\partial}{\partial x}\left[d_{12} \left(\frac{\partial u}{\partial x} + d_{22} \frac{\partial v}{\partial y} \right) \right] = f_y - \rho \frac{\partial^2 v}{\partial t^2} \tag{15}$$

To develop a variational statement corresponding to the problem boundary value, we consider the following alternative problem. Form the governing differential equations, u and $v \in H_1(\Omega)$ can be found for all the weights functions ω_1 and $\omega_2 \in H_0^1(\Omega)$, then all the boundary conditions are satisfied, having:

$$\begin{aligned} 0 = \int_\Omega & \left[\frac{\partial \omega_2}{\partial x}\left(d_{11} \frac{\partial u}{\partial x} + d_{12} \frac{\partial v}{\partial y} \right) + \frac{\partial \omega_2}{\partial y} d_{33} \left(\frac{\partial u}{\partial y} + \frac{\partial v}{\partial x} \right) - \omega_1 f_x + \rho \omega_1 \frac{\partial^2 u}{\partial t^2} \right] dx dy \\ & - \phi_\Gamma \omega_1 \left[\frac{\partial \omega_2}{\partial x} d_{11} \left(\frac{\partial u}{\partial x} + d_{12} \frac{\partial v}{\partial y} \right) n_x d_{33} + \left(\frac{\partial u}{\partial y} + \frac{\partial v}{\partial x} \right) n_y \right] ds \end{aligned} \tag{16}$$

$$0=\int_{\Omega}\left[\frac{\partial\omega_2}{\partial x}d_{33}\left(\frac{\partial u}{\partial y}+\frac{\partial v}{\partial x}\right)+\frac{\partial\omega_2}{\partial y}\left(d_{12}\frac{\partial u}{\partial x}+d_{22}\frac{\partial v}{\partial y}\right)-\omega_2 f_y+\rho\omega_2\frac{\partial^2 v}{\partial t^2}\right]dxdy$$
$$-\phi_\Gamma\omega_2\left[d_{33}\left(\frac{\partial u}{\partial y}+\frac{\partial v}{\partial x}\right)n_x+\left(d_{12}\frac{\partial u}{\partial x}+d_2\frac{\partial v}{\partial y}\right)n_y\right]ds \quad (17)$$

The above numerical problem can be solved using the finite dimensional subspace. By choose *N*-dimensional subspace of $H_h \in H_1(\Omega)$ for *u* and *v* and the test functions ω_1 and ω_2. Let $\{\psi_j\}_{j=1}^{N}=1$, be the basis function of H_h, then:

$$u(x,u,t)=\sum_{j=1}^{N}\varphi_j(x,y)u_j(t) \quad (18)$$

$$v(x,u,t)=\sum_{j=1}^{N}\varphi_j(x,y)v_j(t) \quad (19)$$

$$\omega_1(x,u,t)=\sum_{j=1}^{N}\varphi_j(x,y)\omega_{1j}(t) \quad (20)$$

$$\omega_2(x,u,t)=\sum_{j=1}^{N}\varphi_j(x,y)\omega_{2j}(t) \quad (21)$$

By substitute Eqs. (18) to (21) into Eqs. (16) to (17), and the resulting algebraic equations writing in the matrix form, then the system of ordinary differential equation obtained:

$$M\ddot{U}+A(U)U=F \quad (22)$$

Eq. (22) is a nonlinear system and can be solved by quasi-Newton method.

3 RESULTS AND DISCUSSION

3.1 Physical and mechanical properties

The physical and mechanical properties of the natural femur bone, which is contains of two composites; the outer cortical bone (compact) and the inner cancellous bone (trabecular) structure, are given in Table 2. [29] The effect of the fabrication input parameters i.e. the Nano ceramic filler Powder Compositions, the used compression pressures and hot-pressed temperatures on the mechanical and physical properties for the both fabricated two Nano composites systems TiO_2/ HDPE and TiO_2/ Y_2O_3- partial stabilized zirconia (Y-PSZ)/ HDPE are illustrating in Table 3 and 4, respectively.

In the present work, the experiments were designed by using the full factorial method (FFM), the response surface methodology (RSM) and the analysis of variance (ANOVA) technique to analyze the results. The three level factorial ANOVA analyses using the quadratic design model was implemented for analyzing the effect of input parameters on the compression fracture strength resulting for all the fabricated nanobiocomposites systems are given in Table 5. The model *F*-value of 143.38 and the *P*-values less than 0.0500 implies that the model is significant.

Table 2
The physical and mechanical properties of the natural femur bone.

Sp. composition	Density (g/cm^3)	Modulus of elasticity (*GPa*)	Tensile strength (*MPa*)	Compressive strength (*MPa*)	Fracture strength (*MPa*)	Micro-Vickers Hardness Hv (kg/mm^2)
Cortical bone (compact)	1.6	17.5	208	195	131-224	33
Cancellous bone (trabecular)	2.08	0.1	50–100	68	50–100	66

Table 3
The effect of input parameters on the physical and mechanical properties of the fabricated Nano composites system TiO2/ HDPE.

Exp. No.	Nano ceramic filler Powder Composition	Compounding pressure (*MPa*)	Hot pressed temperature (°*C*)	Compression fracture strength (*MPa*)	Micro-Vickers Hardness Hv (kg/mm^2)	Bulk density (gm/mm^3)	True porosity (%)	Stress Safety Factor
1	1 (%) TiO_2	30	180	26	85.6	0.812	17.38	0.5238
2	1 (%) TiO_2	30	190	27	85.9	0.822	16.36	0.5744
3	1 (%) TiO_2	30	200	27.5	86.1	0.841	14.43	0.5851
4	1 (%) TiO_2	60	180	27.8	86.8	0.833	15.24	0.5914
5	1 (%) TiO_2	60	190	28.3	87.5	0.85	13.51	0.6021
6	1 (%) TiO_2	60	200	28.9	88.4	0.853	13.21	0.6149
7	1 (%) TiO_2	90	180	29.3	88.8	0.866	11.88	0.6234
8	1 (%) TiO_2	90	190	29.8	89.2	0.872	11.27	0.6340
9	1 (%) TiO_2	90	200	30.02	89.65	0.881	10.36	0.6387
10	5 (%) TiO_2	30	180	32.5	87.4	1.041	6.55	0.6915
11	5 (%) TiO_2	30	190	32.8	87.9	1.044	6.28	0.6978
12	5 (%) TiO_2	30	200	33	88.42	1.0471	6.01	0.7020
13	5 (%) TiO_2	60	180	34.2	88.96	1.0481	5.92	0.7275
14	5 (%) TiO_2	60	190	34.9	89.2	1.0492	5.82	0.7426
15	5 (%) TiO_2	60	200	35	89.8	1.0497	5.77	0.7446
16	5 (%) TiO_2	90	180	35.5	90.12	1.051	5.57	0.7553
17	5 (%) TiO_2	90	190	36	90.34	1.0533	5.45	0.7658
18	5 (%) TiO_2	90	200	37	90.57	1.056	5.21	0.7871
19	10 (%) TiO_2	30	180	36.8	89.1	1.126	11.89	0.7828
20	10 (%) TiO_2	30	190	37.03	89.42	1.127	11.82	0.7878
21	10 (%) TiO_2	30	200	38.1	89.76	1.1276	11.77	0.8106
22	10 (%) TiO_2	60	180	37.8	90.22	1.129	11.66	0.8041
23	10 (%) TiO_2	60	190	38.4	90.43	1.136	11.11	0.8169
24	10 (%) TiO_2	60	200	38.9	90.81	1.1374	11.00	0.8276
25	10 (%) TiO_2	90	180	38.6	91.1	1.1379	10.96	0.8211
26	10 (%) TiO_2	90	190	38.9	91.7	1.142	10.64	0.8274
27	10 (%) TiO_2	90	200	39	92.23	1.164	8.92	0.8296

Table 4
The effect of input parameters on the physical and mechanical properties of the fabricated Nano composites system TiO_2/ Y_2O_3-partial stabilized zirconia (Y-PSZ)/ HDPE.

Exp. No.	Nano ceramic fillers Powders Compositions	Compounding pressure (*MPa*)	Hot pressed temperature (°*C*)	Compression fracture strength (*MPa*)	Micro-Vickers Hardness Hv (kg/mm^2)	Bulk density (gm/mm^3)	True porosity (%)	Stress Safety Factor
1	1% TiO_2+2% ZrO_2	30	180	28	90	1.022	13.53	0.5641
2	1% TiO_2+2% ZrO_2	30	190	30	90.5	1.053	10.91	0.6044
3	1% TiO_2+2% ZrO_2	30	200	31	92	1.066	9.81	0.6245
4	1% TiO_2+2% ZrO_2	60	180	32	92.6	1.089	7.87	0.6447
5	1% TiO_2+2% ZrO_2	60	190	33	94	1.104	6.60	0.6648
6	1% TiO_2+2% ZrO_2	60	200	35	95	1.107	6.35	0.7051
7	1% TiO_2+2% ZrO_2	90	180	36	97	1.114	5.75	0.7253
8	1% TiO_2+2% ZrO_2	90	190	37	98	1.116	5.58	0.7454
9	1% TiO_2+2% ZrO_2	90	200	39	99	1.117	5.50	0.7857
10	5% TiO_2+2% ZrO_2	30	180	40	99.5	1.251	7.35	0.8059
11	5% TiO_2+2% ZrO_2	30	190	41	100	1.1233	7.41	0.8260
12	5% TiO_2+2% ZrO_2	30	200	41.5	100.56	1.125	7.27	0.8361
13	5% TiO_2+2% ZrO_2	60	180	42.3	100.88	1.127	7.11	0.8522
14	5% TiO_2+2% ZrO_2	60	190	43	101	1.129	6.94	0.8663
15	5% TiO_2+2% ZrO_2	60	200	44	101.47	1.133	6.61	0.8864
16	5% TiO_2+2% ZrO_2	90	180	45.6	102	1.14	6.34	0.9187
17	5% TiO_2+2% ZrO_2	90	190	46.2	104	1.152	5.05	0.9308
18	5% TiO_2+2% ZrO_2	90	200	47	106	1.157	4.63	0.9469
19	10% TiO_2+2% ZrO_2	30	180	47.3	107	1.233	10.47	0.9529
20	10% TiO_2+2% ZrO_2	30	190	47.8	109	1.245	9.60	0.9630
21	10% TiO_2+2% ZrO_2	30	200	47.92	110	1.246	9.53	0.9655
22	10% TiO_2+2% ZrO_2	60	180	48	112	1.251	9.16	0.9670
23	10% TiO_2+2% ZrO_2	60	190	48.4	113	1.277	7.28	0.9751
24	10% TiO_2+2% ZrO_2	60	200	48.7	115	1.311	4.81	0.9811
25	10% TiO_2+2% ZrO_2	90	180	49	117.5	1.323	3.94	0.9872
26	10% TiO_2+2% ZrO_2	90	190	49.45	118	1.344	2.41	0.9963
27	10% TiO_2+2% ZrO_2	90	200	50	120	1.352	1.83	1.0073

Table 5
The ANOVA analysis of the compression fracture strength for all the fabricated nanobiocomposites system.

Source	Sum of Squares	d_f	Mean Square	*F*-value	*P*-value	
Model	463.61	3	154.54	143.38	< 0.0001	significant
A-Nano ceramic filler Powder Composition	428.79	1	428.79	397.84	< 0.0001	
B-Compounding pressure	30.39	1	30.39	28.20	< 0.0001	
C-Hot pressed temperature	4.42	1	4.42	4.10	0.0546	
Residual	24.79	23	1.08			
Cor Total	488.39	26				

The ANOVA analyses used the quadratic design model for analyzing the effect of input parameters on the bulk densities responses values resulting for all the fabricated TiO2/HDPE Nanobiocomposites system as given in Table 6. The model *F*-value of 620.73 and the *P*-values less than 0.0500 implies that the model is also significant.

The final equations for prediction about the bulk density responses values without further experimental work in terms of actual factors for the both fabricated TiO_2/HDPE and TiO_2+2 % ZrO_2/HDPE Nano ceramic fillers Compositions systems are:

Bulk density (I) = + 0.817720+0.083660* TiO_2 Nano ceramic fillers contain (%) - 0.000109* Compounding pressure (*MPa*) - 0.001478* Hot pressed temperature (°*C*) (23)

Bulk density (II) = + 0.937383+0.022374 * TiO_2+2% ZrO_2 Nano filler contain (%) + 0.000835* Compounding pressure (*MPa*) + 0.000356 * Hot pressed temperature (°*C*) (24)

The effect of input parameters on the bulk densities values for all the fabricated TiO_2/HDPE and TiO_2+ 2 % ZrO2/HDPE Nano ceramic fillers Compositions systems are shown in the 3D graphs of Fig. 1. These graphs show that the bulk densities values were increased with increasing the process parameters, i.e. Nano ceramic filler contain, the compounding pressure and the hot-pressed temperature. With the increase of the TiO_2 filler contain from 1% to 10 %, the value increase by 30.24 %. When using 10% TiO_2 with adding 2% partial stabilized zirconia (Y-PSZ), hot pressed temperature of 200 °*C* and compounding pressure of 90 *MPa*, this value is further increase by 13.91%. The reasons for this increase in the bulk densities values is that the added ceramic Nano filler materials have four to five times the density of the high-density polyethylene (HDPE) matrix and the excellent bonding between their particles.

Table 6
The ANOVA analysis of the bulk densities responses for all the TiO_2/HDPE Nanobiocomposites system.

Source	Sum of Squares	d_f	Mean Square	*F*-value	*P*-value	
Model	0.3983	9	0.0443	620.73	< 0.0001	significant
A-TiO_2 Nano ceramic fillers Powders Compositions	0.3747	1	0.3747	5254.80	< 0.0001	
B-Compounding pressure	0.0030	1	0.0030	41.51	< 0.0001	
C-Hot pressed temperature	0.0007	1	0.0007	9.65	0.0064	
AB	0.0005	1	0.0005	6.56	0.0202	
A^2	0.0316	1	0.0316	443.79	< 0.0001	
Residual	0.0012	17	0.0001			
Cor Total	0.3995	26				

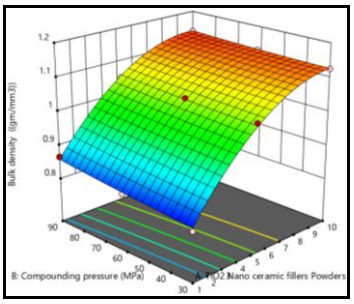

(a) Hot pressed temperature (180 °*C*)

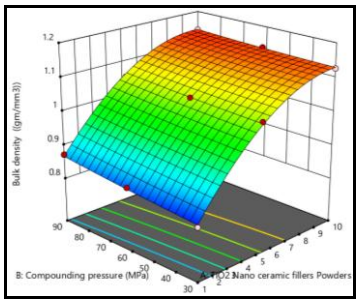

(b) Hot pressed temperature (190 °*C*)

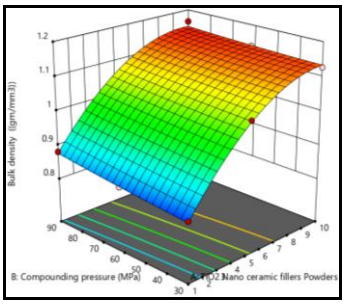

(c) Hot pressed temperature (200 °*C*)

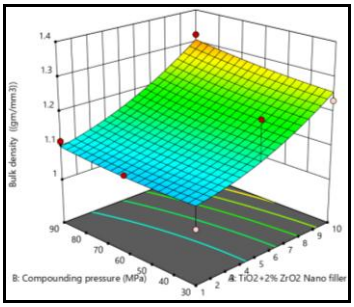

(d) Hot pressed temperature (180 °*C*)

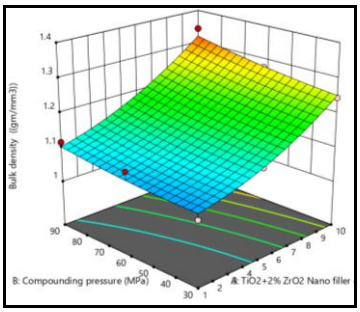

(e) Hot pressed temperature (190 °*C*)

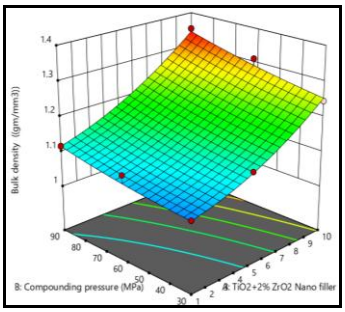

(f) Hot pressed temperature (200 °*C*)

Fig.1
The 3D graphs for the effect of input parameters on the bulk densities values for all the fabricated TiO_2/HDPE and TiO_2+ 2 % ZrO_2/HDPE Nano ceramic fillers Compositions systems.

The effect of compression fracture strengths and the Nano ceramic fillers contains on the bulk densities values for the fabricated TiO_2/HDPE and TiO_2 +2 % ZrO_2/HDPE Nano composites systems are shown in Fig. 2 (a) and (b), respectively. The bulk densities values were increased with increasing the compression fracture strength and the Nano ceramic filler contain, reached its maximum values as 1.164 kg/mm^2 for the first Nano Compositions system and with the adding of 2% partial stabilized zirconia (Y-PSZ) this value increased to1.352, i.e. increased by 13.91 %.

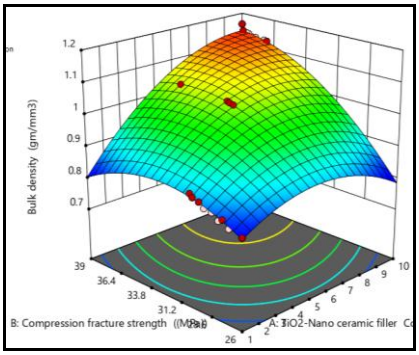

(a) Fabricated system (I) / TiO_2/HDPE Nano composites

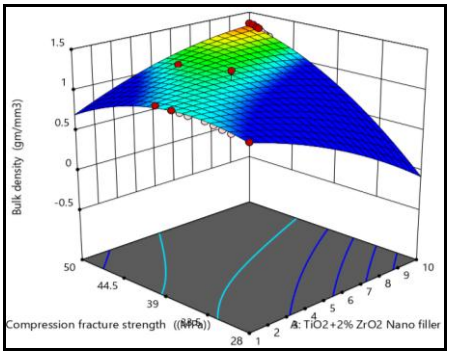

(b) Fabricated system (II) / TiO_2 +2 % ZrO_2/HDPE Nano composites

Fig.2
The effect of compression fracture strength and the Nano ceramic fillers contains on the bulk densities values.

The reason for this increase in the bulk densities values is the increase of the ceramic Nano filler contents added to the fabricated biomaterials systems. These Nano ceramic materials with their high densities values and their high correlation with the molecules of the matrix under high pressure and heat produced a high strengths and densities biocomposities materials closed to the specifications of human natural bone, making them at the forefront of materials in the processes of grafting and repair bones operations. The final prediction equations for the effect of

compression fracture strength and the Nano ceramic fillers contains on the bulk densities values for the both fabricated compositions systems are:

Bulk density (I) = - 0.975668 - 0.036289 *TiO_2 Nano ceramic filler Composition + 0.113936 * Compression fracture strength (*MPa*) (25)

Bulk density (II) = + 0.986515 + 0.018955 * TiO_2+2% ZrO_2 Nano filler contain + 0.002076 * Compression fracture strength (*MPa*) (26)

The final prediction equations for the true porosities responses values for the both fabricated TiO_2/HDPE and TiO_2+ 2 % ZrO_2/HDPE Nano ceramic fillers compositions systems are:

True porosity (I) = + 21.50085 - 5.52285 * TiO_2 Nano ceramic fillers contain (%) - 0.027231* Compounding pressure + 0.080767* Hot pressed temperature (27)

True porosity (II) = + 28.84149 - 0.152086 *TiO_2+2% ZrO_2 Nano filler contain-0.083056* Compounding pressure - 0.084333 *Hot pressed temperature (28)

Fig. 3 shows the effect of input parameters on the percentages values of true porosity for all the fabricated TiO_2/HDPE and TiO_2+ 2 % ZrO2/HDPE Nano bio compositions systems. These graphs show that the percentages true porosity values were decreased with increasing the process parameters, i.e. Nano ceramic filler contain, the compounding pressure and the hot-pressed temperature. With the increase of the TiO_2 filler ceramic contain from 1% to 10 %, the value percentages true porosity decreases by 48.68 %. When using 10% titanium oxide Nano ceramic powder (TiO_2) with adding 2% partial stabilized zirconia (Y-PSZ), hot pressed temperature of 200 °*C* and compounding pressure of 90 *MPa*, this value is further decrease by 84.85 %, i.e. the percentages true porosity values were decreased from 17.38 % to the minimum value of 1.83 %. These figures show also that the addition of a small percentage of partial stabilized zirconia (Y-PSZ) led to stability of the true porosity values with increasing the TiO_2 filler ceramic contain proportion as shown in the Fig. 3 (d), (e) and (f). These results are evidence of a remarkable degree of porosity of the produced Nano biomaterials for orthopedic that are appropriate to the various patient's clinical conditions and the degree of osteoporosis. The reason for this low degree of percentages values of true porosity obtained, which is very close to the natural human bones properties, is the use of nanomaterials in the fabricating and secondly in the same fabricating process by using the hot nanoparticles powder pressed method instead of the traditional melting methods.

Fig. 4 shows the effect of compression fracture strength obtained from experimental results and the Nano ceramic fillers contains on the percentages values of true porosity for all the fabricated Nano compositions systems. The percentages true porosity values were decreased with increasing the compression fracture strength and the Nano ceramic filler contain reached its minimum values as 8.92 % for the first TiO_2/HDPE Nano Compositions system. With the adding of 2% partial stabilized zirconia (Y-PSZ) with the maximum compression fracture strength as shown in Fig. 4 (b), this value true porosity was decreased to 1.83 %, i.e. reduced by 84.85 % and these results were obtained duo to the good densification process during the liquid phase sintering stage.

The obtained values of the compression fracture strength show that these values were increased with increasing the process parameters, i.e. Nano ceramic filler contain the compounding pressure and the hot-pressed temperature. With the increase of the TiO_2 filler ceramic contain from 1% to 10 %, the value of the compression fracture strength increased by 33.34 %. When using 10% titanium oxide Nano ceramic powder (TiO_2) with adding 2% partial stabilized zirconia (Y-PSZ), hot pressed temperature of 200 °*C* and compounding pressure of 90 *MPa*, this value is further increased by 22 %. In a previous study on investigated the injection molded 5 % TiO_2/ HDPE nanocomposites, the maximum compression strength it reached to 26.3 *MPa* [15]), while for PEEK femoral component is 30 *MPa* [30], and equal to 12.5 *MPa* achieved when composite having composition of 70% LDPE+10% TiO_2 +20% Al_2O_3 was used [31], i.e. the maximum compression strength for this study is higher by 90.11% than the previous mentioned studies. The final prediction equations for the effect of compression fracture strength on the true porosities for the both fabricated compositions systems are:

True porosity (I) = + 62.46377 + 1.73782 * TiO_2 Nano ceramic filler Composition - 1.82694 * Compression fracture strength (*MPa*) (29)

True porosity (II) = + 27.60304 + 0.834508 * TiO_2+2% ZrO_2 Nano filler contain - 0.599033 * Compression fracture strength (*MPa*) (30)

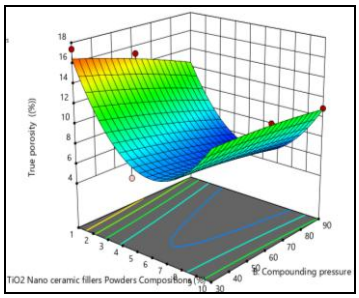

(a) Hot pressed temperature (180 °*C*)

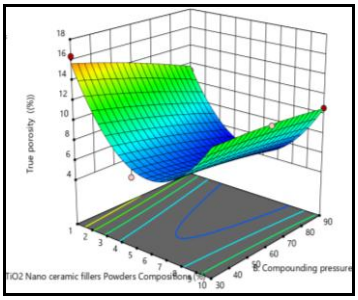

(b) Hot pressed temperature (190 °*C*)

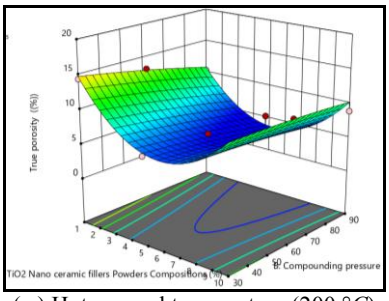

(c) Hot pressed temperature (200 °*C*)

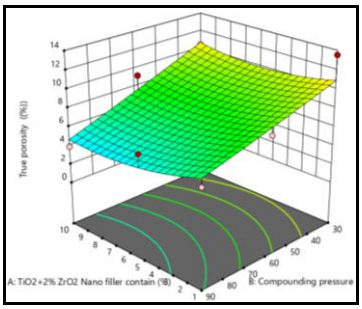

(d) Hot pressed temperature (180 °*C*)

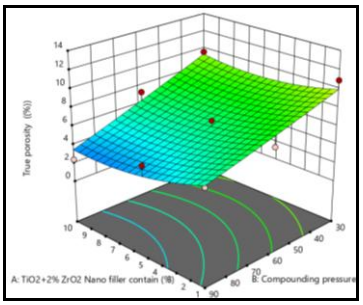

(e) Hot pressed temperature (190 °*C*)

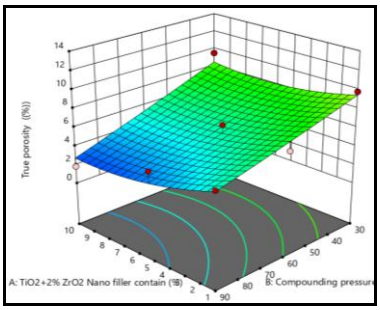

(f) Hot pressed temperature (200 °*C*)

Fig.3
The 3D graphs for the effect of input parameters on the true porosities values for all the fabricated TiO_2/HDPE and TiO_2+ 2 % ZrO_2/HDPE Nano ceramic fillers Compositions systems.

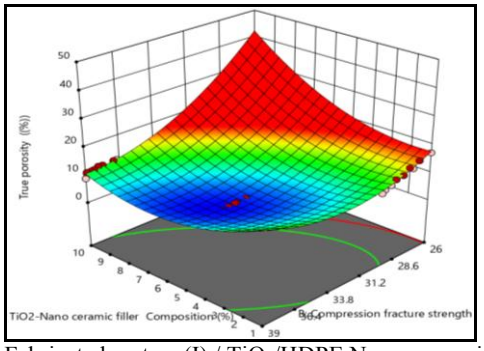

(a) Fabricated system (I) / TiO_2/HDPE Nanocomposites

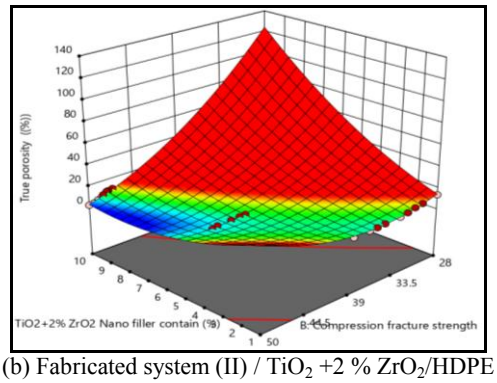

(b) Fabricated system (II) / TiO_2 +2 % ZrO_2/HDPE Nanocomposites

Fig.4
The effect of compression fracture strength and the Nano ceramic fillers contains on the percentages values of true porosity.

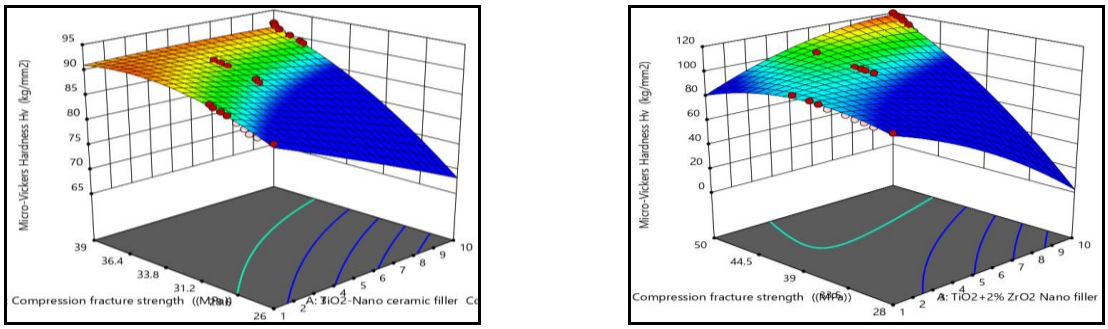

(a) (b)

Fig.5
The effect of compression fracture strength and the Nano ceramic fillers contains on the Vickers micro hardness values; (a) for the fabricated system (I) / TiO2/HDPE Nano composites; (b) for the fabricated system (II) / TiO_2 +2 % ZrO_2/HDPE Nano composites.

Fig. 5 (a) and (b) show the effect of compression fracture strengths and the Nano ceramic fillers contains on the micro-Vickers Hardness values for the both fabricated TiO_2/HDPE and TiO_2 +2 % ZrO_2/HDPE Nano compositions systems, respectively. The micro-Vickers Hardness reached its maximum values with increasing the compression fracture strength and the Nano ceramic filler contain, as 92.23 gm/mm^3 for the first Nano Compositions system. With the adding of 2% partial stabilized zirconia (Y-PSZ) this value increased to120 gm/mm^3, i.e. increased by 30.11 %. The increase in the micro-Vickers Hardness values are due to the increase of the high strengths ceramic Nano filler contents added to the fabricated biomaterials systems. The final prediction equations for the effect of compression fracture strength and the Nano ceramic fillers contains on the micro-Vickers Hardness values for the both fabricated compositions systems are:

Micro-Vickers Hardness (I) = + 9.68811 - 5.47079 * TiO_2 Nano ceramic filler Composition + 4.71726 Compression fracture strength (*MPa*) (31)

Micro-Vickers Hardness (II) = + 70.94106 + 1.11439 * TiO_2+2% ZrO_2 Nano filler contain + 0.628565 * Compression fracture strength (*MPa*) (32)

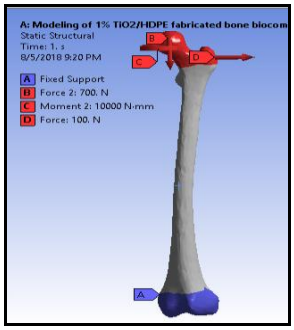

(a) Patient weights 70 *kg*

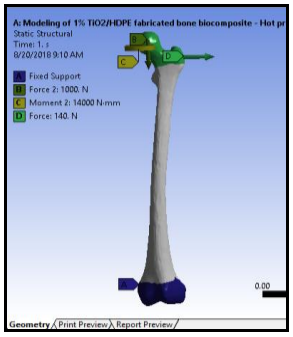

(b) Patient weights 100 *kg*

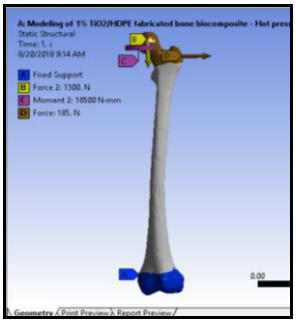

(c) Patient weights 130 *kg*

Fig.6
The boundary conditions for the femur bone ANSYS models for the bodies of patients weights with 70, 100 and 130 *kg*.

3.2 ANSYS modeling for stress distribution

The human femur bone 3D model to simulate the stress and strain fields corresponding to the patient activities was implemented by using the Solid works and analyzed by using the finite element module ANSYS workbench 15.7. The cortical bone is asymmetric and anisotropic in tension and compression. To predicted bone failure and response, an orthotropic symmetric model was recommended utilizes the elastic-plastic constitutive, symmetric and isotropic models [32]. The femur bone mechanical properties for an adult human femur are; density =1.75 gm/cm^3, Young's modulus = 16.7 *GPa*, ultimate tensile strength = 43.5 *MPa*, ultimate compressive strength = 115.3 *MPa* and the Poisson's ratio for both bone layers = 0.3 [1, 24].

The external loads applied at the head of the bone corresponding to periodic cycles of patient's activities with 70, 100 and 130 *kg* body patient weights, respectively (or approximately two times normal body weight). The femur bone head-implant systems was loaded with 700, 1000 and 1300 *N* axial, lateral 100, 140 and 185 *N* loads and torsional moment of 10.0, 14.0 and 18.5 *Nm*. At the lower medial condyle surface of the fixed support is provided and the displacement is restricted in the all direction [23-25, 33].

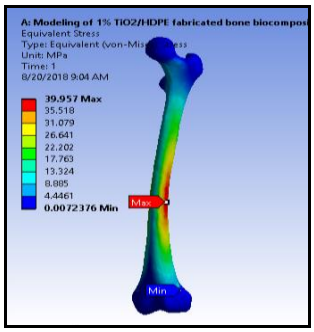

(a) Patient weights 70 *kg*

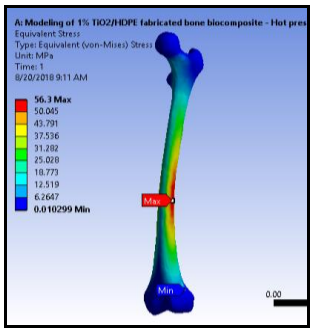

(b) Patient weights 100 *kg*

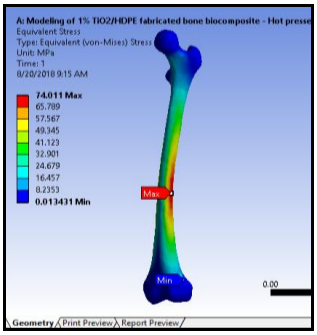

(c) Patient weights 130 *kg*

Fig.7
The maximum equivalent von–Misses Stresses obtained to withstand the patients bodies weights with 70, 100 and 130 *kg*.

The boundary conditions for the femur bone ANSYS models for the bodies of patients weights with 70, 100 and 130 *kg* are shown in Fig. 6 (a), (b) and (c), respectively. The maximum equivalent von –Misses stresses obtained to withstand the highest stresses producing during daily activities for prepared and fabricated Nano composites for bones repairs equal to 39.96, 56.30 and 74.01 *MPa*, which they represent the stresses resulting from the of loads for the above three the bodies of patients weights as shown in Fig. 7 (a), (b) and (c), respectively. The distribution of these stresses shows that the location of maximum equivalent von –Misses stresses, is in the middle portion of the bone with the lowest cross-sectional area where the fractures in various incidents are confirmed by most cases. In a previous study, the implemented femur bone maximum equivalent von –Misses Stresses obtained for axisymmetric loads natural femur bone equal to 29.64 *MPa* [21], and for natural femur bone ranged between 22 *MPa* and 26 *MPa* [9]. This means that the nanocomposites systems produced in the current work withstand higher stresses than the natural bone by 52.65 % and by 34.82 % higher than the previous study just mentioned.

Figs. 8 and 9 show the effect of input parameters for the fabricated Nano composites systems (I) and (II), respectively on the stress safety factors values for different Nano ceramic fillers Powders compositions according to the correspondents equivalent von–Misses stresses resulted from the external loads applied at the head of the bone for patient's activities with 70, 100 and 130 *kg* body patient weights (at 90 *MPa* compounding pressure and 200 °*C* hot pressed temperature), respectively.

As shown in these figures, the value of the stress safety factors was increased with increasing the ceramic filler contains, the hot-pressed temperature and the compounding pressure. The results show that when increasing the Nano ceramic filler contains from 1% to 10 %, the stress safety factors increase by 58.38 %. When adding 2 % of zirconia (ZrO_2), the stress safety factors reached its maximum values, with an additional increase in its value by 21.42 % as shown on the 3D graphs Fig. 10 (a) and (b). The increase in the stress safety factors values can be returned to the adding of the high mechanical properties of the ceramic Nano filler materials and excellent bonding properties with the HDPE polymer matrix.

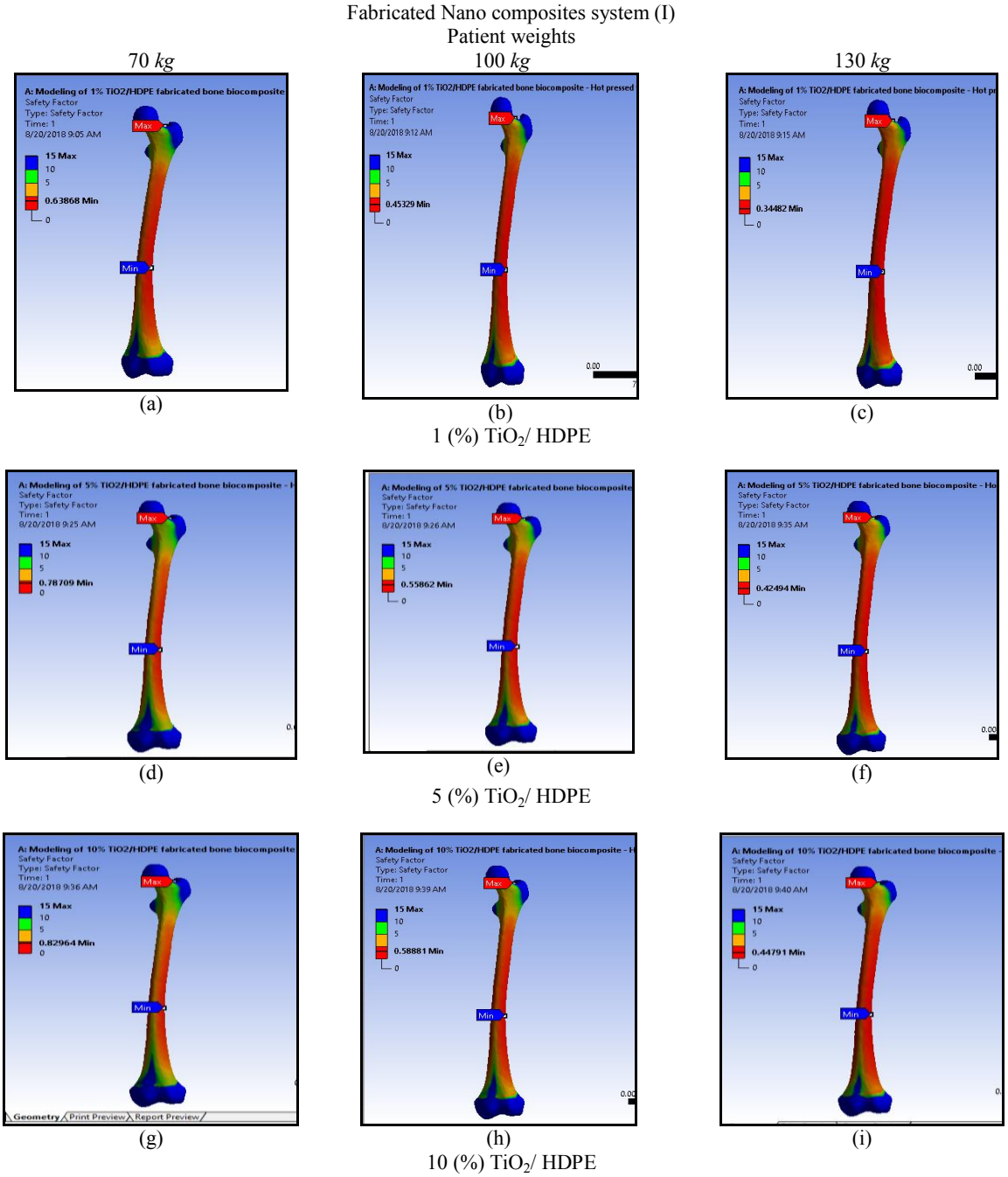

Fig. 8
The effect of the input parameters for the fabricated Nano composites system (I) on the stress safety factors for different Nano ceramic fillers compositions and patient's bodies weights (at 90 *MPa* compounding pressure and 200 °*C* hot pressed temperature).

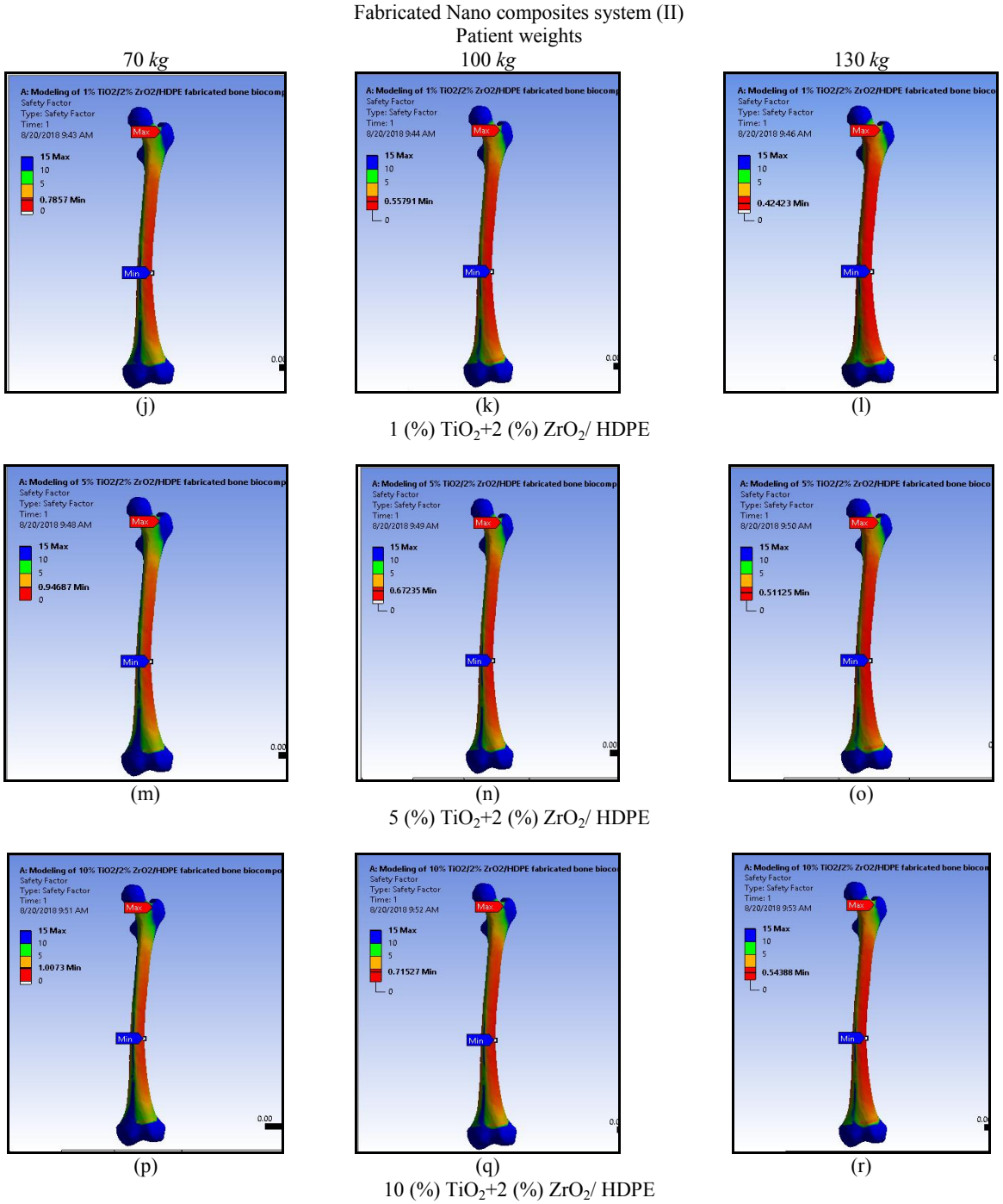

Fig. 9
The effect of the input parameters for the fabricated Nano composites system (I) on the stress safety factors for different Nano ceramic fillers compositions and patient's bodies weights (at 90 *MPa* compounding pressure and 200 °*C* hot pressed temperature).

The final prediction equations for the effect of process input parameters on the stress safety factors values for the both fabricated compositions systems are:

Stress safety factors (I) = + 1.05751 + 0.015519 *TiO_2 Nano filler contain (%) - 0.005765 * Patient weights (33)

Stress safety factors (II) = + 1.28882 +0 .018082* TiO_2+2% ZrO_2 Nano filler contain (%) - 0.007003 * Patient weights (34)

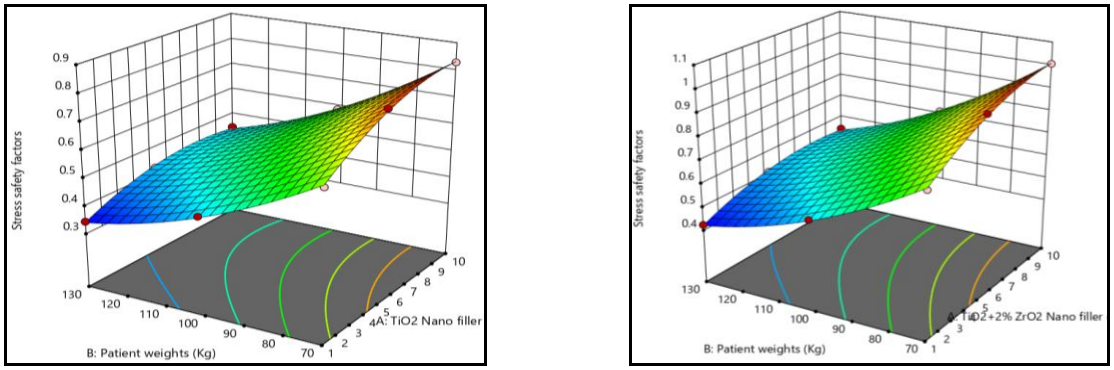

(a) (b)

Fig.10
The 3D graphs for the effect of the input parameters for the fabricated Nano composites systems on the stress safety factors values for different Nano ceramic fillers Powders compositions and patient's weights.

4 CONCLUSIONS

After study and analysis of the effect of all parameters that influences the obtained qualities for the fabricated Nano biocomposities systems, the following conclusions can be drawn:

1- The results show that the bulk densities, the stress safety factors values for all the fabricated TiO_2/HDPE and TiO_2+ 2 % ZrO_2/HDPE Nano ceramic fillers Compositions systems were increased with increasing the process parameters, while the percentages values of true porosity were decreased.

2- With the increase of the TiO_2 filler to 10 %, the value bulk densities increase by 30.24 % and when adding 2% partial stabilized zirconia (Y-PSZ), this value is further increase by 13.91%, i.e. reached its maximum values as 1.164 kg/mm^2 for the first Nano system and to1.352 for the second system, respectively.

3- The percentages true porosity values were decreased with increasing the compression fracture strength reached its minimum values as 8.92 % for the first TiO_2/HDPE Nano Compositions system. With the adding of 2% partial stabilized zirconia (Y-PSZ), this value was decreased to 1.83 %, i.e., these values were decreased by 48.68 % and by 84.85 %, respectively.

4- The obtained values of the compression fracture strength show that these values were increased with increasing the process parameters by 33.34 % for the first fabricated Nano system. When adding 2% partial stabilized zirconia this value is further increased by 22 %. The maximum compression strength for this study is higher by 90.11% than the previous mentioned studies.

5- The micro-Vickers Hardness reached its maximum values with increasing the compression fracture strength, reached 92.23 gm/mm^3 for the first Nano Compositions system. With the adding of 2% partial stabilized zirconia (Y-PSZ) this value increased to120 gm/mm^3, i.e. increased by 30.11 %.

6- The maximum equivalent von –Misses Stresses obtained from ANSYS models equal to 39.96, 56.30 and 74.01 *MPa*, resulting from the three bodies of patients weights and the nanocomposites systems produced in the current work withstand higher stresses than the natural bone by 52.65 higher than the previous studies.

7- The results show that when increasing the Nano ceramic filler contains from 1% to 10 %, the stress safety factors increase by 58.38 %. When adding 2 % of zirconia (ZrO_2), the stress safety factors reached its maximum values, with an additional increase in its value by 21.42 %.

REFERENCES

[1] Zagane M.E., Benbarek S., Sahli A., Bachir B., Serier B., 2016, Numerical simulation of the femur fracture under static loading, *Structural Engineering and Mechanics* **60**(3): 405-412.

[2] Pedro H.C., Kestur G., Fernando W., 2009, Nanocomposites: synthesis, structure, properties and new application opportunities, *Materials Research* **12**(1): 1-39.

[3] Luca C., Fulvia T., Massimiliano B., Fabio B., Susanna S., Marco V., 2008, Multiscale investigation of the functional properties of the human femur, *Philosophical Transactions of the Royal Society A* **366**: 3319-3341.

[4] Abdel-Wahab A.A., Maligno A.R., Silberschmidt V.V., 2012, Micro-scale modelling of bovine cortical bone fracture: analysis of crack propagation and microstructure using X-FEM, *Computational Materials Science* **52**(1): 128-135.

[5] Adeel A., 2014, Implantable zirconia bioceramics for bone repair and replacement: A chronological review, *Materials Express* **4**(1): 1-12.

[6] Jenan S.K., Huseein G., 2017, The development of biomimetic nano $CaCO_3$/ PPBio composites as bone repair materials- optimal thermal properties evaluation, *Journal of Babylon University, Engineering Sciences* **25**(5): 1562-1571.

[7] Toktam G., Azadeh S., Mohammad H.E., Alireza M., Jebraeel M., Ali M., 2018, Current concepts in scaffolding for bone tissue engineering, *The Archives of Bone and Joint Surgery* **6**(2): 90-99.

[8] Sergey V.D., 2011, Biocomposites and hybrid biomaterials based on calcium orthophosphates, *Biomatter* **1**(1): 3-56.

[9] Mohamed T., Emmanuel R., Patrick C., Christian H., Martine P., Sylvie W.M., 2008, Numerical modeling of an osteoporotic femur: comparison before and after total hip prosthesis implantation, *European Journal of Computational Mechanics* **17**(5,6,7): 785-793.

[10] Nackenhorst U., 1997, Numerical simulation of stress stimulated bone remodeling, *Technische Mechanik* **7**(1): 31-40.

[11] Abdul Kaleel S.H., Bahuleyan B. Ko., Masihullah J., Mamdouh A., 2011, Thermal and mechanical properties of polyethylene/doped-TiO_2 nanocomposites synthesized using in situ polymerization, *Journal of Nanomaterials* **964353**: 1-6.

[12] Rajkamal B., Sivakumar S., Naveen N., 2014, Bioceramic nanofibres by electrospinning, *Fibers* **2**: 221-239.

[13] Wen S., Mohammad S.M., Hui Z., Jesse Z., Hiran P., 2012, MTA-enriched nanocomposite TiO_2-polymeric powder coatings support human mesenchymal cell attachment and growth, *Biomedical Materials* **7**: 1-12.

[14] Lennon A.B., Prendergast P.J., 2002, Residual stress due to curing can initiate damage in porous bone cement: experimental and theoretical evidence, *Journal of Biomechanics* **35**: 311-321.

[15] Abdel-Hamid I.M., Mohammad S.M., Anusha M., Hifsa P., Uma M.K., 2017, On the injection molding processing parameters of HDPE-TiO_2 nanocomposites, *Materials* **10**(85): 1-25.

[16] Shariati M., Hatami H., Eipakchi H. R., Yarahmadi H., Torabi H., 2011, Experimental and numerical investigations on softening behavior of POM under cyclic strain-controlled loading, *Polymer-Plastics Technology and Engineering* **50**(15): 1576-1582.

[17] Hatami H., Hosseini M., Yasuri A. K., 2019, Perforation of thin aluminum targets under hypervelocity impact of aluminum spherical projectiles, *Materials Evaluation* **77**(3): 411-422.

[18] Rad M.S., Hatami H., Alipouri R., Nejad A.F., Omidinasab F., 2019, Determination of energy absorption in different cellular auxetic structures, *Mechanics & Industry* **20**(3): 1-11.

[19] Rad M.S., Hatami H., Ahmad Z., Yasuri A.K., 2019, Analytical solution and finite element approach to the dense re-entrant unit cells of auxetic structures, *Acta Mechanica* **230**: 2171-2185.

[20] Hatami H., Shariati M., 2019, Numerical and experimental investigation of SS304L cylindrical shell with cutout under uniaxial cyclic loading, *Iranian Journal of Science and Technology, Transactions of Mechanical Engineering* **43**:139-153.

[21] Ahmet C.C., Vahdet U., Recep K., 2007, Three-dimensional anatomic finite element modelling of hemi-arthroplasty of human hip joint, *Trends in Biomaterials and Artificial Organs* **21**(1): 63-72.

[22] Senthil Maharaja P.S.R., Maheswaranb R., Vasanthanathan A., 2013, Numerical analysis of fractured femur bone with prosthetic bone plates, *Procedia Engineering* **64**: 1242-1251.

[23] Dmitry I., Yuri B., Anatoly B., 2016, A numerical comparative analysis of ChM and Fixion nails for diaphyseal femur fractures, *Acta of Bioengineering and Biomechanics* **18**(3): 73-81.

[24] Srimongkol S., Rattanamongkonkul S., Pakapongpun A., Poltem D., 2012, Mathematical modeling for stress distribution in total hip arthroplasty, *International Journal of Mathematical Models and methods in Applied Sciences* **6**(7): 885-892.

[25] Aleksa M., Aleksandar S., Katarina C., Uros T., Branislav D., 2017, Numerical analysis of stress distribution in total hip replacement implant, *Integritet I Vek Konstrukcija* **17**(2): 139-144.

[26] Sajad A.K., 2013, The fatigue design of a bone preserving hip implant with functionally graded cellular material, *Damiano Pasini Journal of Medical Devices* **7**: 1-2.

[27] Jenan S.K., 2014, Preparation and Characterization of Hydroxyapatite/ Yttria Partially Stabilized Zirconia Polymeric Biocomposite, PhD. Thesis, Department of Production Engineering and Metallurgy- University of Technology, Baghdad, Iraq.

[28] Amin D.T., Jafar T.A., Jenan S.K., 2014, Effect of particle size on the physical and mechanical properties of nano HA/HDPE bio-composite for synthetic bone substitute, *Engineering and Technology Journal* **32**(2): 286-297.

[29] Kashan J.S., Rija N.H., Abbas T.A., 2017, Modified polymer matrix nano biocomposite for bone repair and replacement- radiological study, *Engineering and Technology Journal* **35**(2): 365-371.

[30] Lennert R., Dennis J., Adam B., Nico V., 2017, The mechanical response of a polyetheretherketone femoral knee implant under a deep squatting loading condition, *Proceedings of the Institution of Mechanical Engineers, Part H ,Journal Engineering in Medicine* **231**(12): 1204-1212.

[31] Dhabale R., Jatti V.S., 2016, A bio-material: mechanical behaviour of LDPE-Al_2O_3-TiO_2, *Materials Science and Engineering* **149**: 1-10.

[32] Khor F., Cronin D.S., Watson B., Gierczycka D., Malcolm S., 2018, Importance of asymmetry and anisotropy in predicting cortical bone response and fracture using human body model femur in three-point bending and axial rotation, *Journal of the Mechanical Behavior of Biomedical Materials* **87**: 213-229.

[33] Bartosz N., Jerzy N., 2006, Numerical simulation of influence of chosen parameters on tensile stresses in bone cement layer in total hip arthoplastry, *Advanced in Materials Science E* **6**(2): 9-17.